Parametrizations of triaxial deformation and $E2$ transitions of the wobbling band

Yoshifumi R. Shimizu,[1] Takuya Shoji,[1] and Masayuki Matsuzaki[2]
[1]*Department of Physics, Graduate School of Sciences, Kyushu University, Fukuoka 812-8581, Japan*
[2]*Department of Physics, Fukuoka University of Education, Munakata, Fukuoka 811-4192, Japan*
(Received 25 July 2007; published 29 February 2008)

There are various different definitions for the triaxial deformation parameter "γ". It is pointed out that the parameter conventionally used in the Nilsson (or Woods-Saxon) potential, γ(pot:Nils) [or γ(pot:WS)], is not appropriate for representing the triaxiality γ defined in terms of the intrinsic quadrupole moments. The difference between the two can be as large as a factor two in the case of the triaxial superdeformed bands recently observed in Hf and Lu nuclei, i.e., γ(pot:Nils) $\approx 20^\circ$ corresponds to $\gamma \approx 10^\circ$. In our previous work, we studied the wobbling excitations in Lu nuclei using the microscopic framework of the cranked Nilsson mean-field and the random phase approximation. The most serious problem was that the calculated $B(E2)$ value is about factor two too small. It is shown that the origin of this underestimate can mainly be attributed to the small triaxial deformation parameter $\gamma \approx 10^\circ$ that corresponds to γ(pot:Nils) $\approx 20^\circ$. If the same triaxial deformation parameter is used as in the analysis of the particle-rotor model, $\gamma \approx 20^\circ$, the calculated $B(E2)$ gives correct magnitude of the experimental data.

DOI: 10.1103/PhysRevC.77.024319 PACS number(s): 21.10.Re, 21.60.Jz, 23.20.Lv, 27.70.+q

I. INTRODUCTION

The triaxial deformation of atomic nuclei has been one of the longstanding issues in nuclear structure physics. The triaxial rotor model was first introduced by Davydov-Filippov [1], and has been proved to be very useful for the study of the spectra of odd transitional nuclei [2]. More recently, the model-independent sum-rule method [3] has been used to analyze the Coulomb excitation of the quadrupole collective motion, the triple $E2$ matrix elements of which are related to the the triaxiality parameter γ. Many of the Coulomb excitation measurements have revealed clearly nonaxial deformation [4], although it has been difficult to determine whether the nonaxiality is of static or of dynamic nature. It has been expected that the effect of triaxial deformation appears more explicitly in high-spin states. For example, the so-called signature staggering of the excitation energies and/or the $M1/E2$ transition probabilities in odd or odd-odd nuclei has been expected to be a good indicator of triaxiality, see Refs. [5,6] and references therein. The result of analyses has not been so conclusive.

The situation, however, changed quite recently: The nuclear wobbling motion [7] has been identified in Lu isotopes, ^{163}Lu [8–11], ^{165}Lu [12], ^{167}Lu [13], and ^{161}Lu [14]. These observations indicate that the triaxiality is of static nature, and one can study the rotational motion of triaxially deformed nucleus. In fact it had been predicted that the strong triaxial deformation would appear in the Hf and Lu mass region [15,16]. The measurements of wobbling phonon excitations mentioned above were made in this region. The triaxial deformation predicted in such nuclei is the so-called positive γ shape in the Lund convention [17], i.e., nuclei rotate about the shortest axis, and the associated rotational sequence is called the triaxial superdeformed (TSD) band [18–20]. In order to pin down how much the TSD nucleus deforms triaxially, it is crucial to measure the $E2$ transition probabilities. The measurements of the $B(E2)$ [21,22] of not only in-band (intraband), but also out-of-band (interband) transitions of the states in the yrast TSD band and those in the excited wobbling band are necessary to obtain the information about the triaxial deformation. The detailed study using the particle-rotor model [8,23,24], with an odd $i_{13/2}$ proton coupled to the triaxial rotor, which is suitable for the description of odd Lu TSD bands, revealed that the observed ratio of the out-of-band to the in-band $B(E2)$'s, $B(E2)_{\rm out}/B(E2)_{\rm in}$, is consistent with the triaxiality parameter $\gamma \approx +20^\circ$.

It should, however, be noted that the conventional rotor model [1] with irrotational moments of inertia has an essential problem: The rotor rotates around the intermediate axis, which corresponds to the negative γ shape, and is inconsistent with the measured $B(E2)$ ratio. In order to avoid this problem and to simulate the positive γ shape, the largest and intermediate moments of inertia are interchanged in Refs. [8,23,24]. We have studied the wobbling motion in the Lu region [25–27] by employing a microscopic framework, the cranked mean-field and the random phase approximation (RPA) [28–30], by which three moments of inertia corresponding to the positive γ shape are naturally obtained. This approach is suitable for describing the vibrational excitations in the rapidly rotating nuclei, see, e.g., Refs. [31–35]. It was used to study possible wobbling excitations in normal deformed nuclei in our previous works [36,37], and more recently in Refs. [38,39]. The instability of the wobbling excitation was also studied [40] in relation to the tilted axis cranking rotation.

In our previous studies [25–27], the RPA solutions that could be nicely interpreted as wobbling phonons were found in the Lu region for a suitable range of deformation parameters corresponding to the prediction of the TSD bands. The calculated excitation energies were in a reasonable range in comparison with the experimental data. However, the calculated $B(E2)$ ratios were systematically too small by about a factor two to three, as long as the triaxiality parameters predicted by the Nilsson-Strutinsky calculations [19,20] were used. The main purpose of the present work is to discuss

why our RPA calculations underestimated the $B(E2)$ ratio. In the course of the discussion, it is clarified that the parameter γ conventionally used does not accurately represent the triaxiality of the geometric shape, and one has to be very careful when one talks about the triaxial deformation, in particular large ones in the case of TSD bands.

As for the fundamental question of whether the triaxiality is of static or of dynamic nature, i.e., whether the γ-soft or γ-rigid model is valid, it was maintained in Ref. [41] that the out-of-band $B(E2)$ from the one-phonon wobbling band is not enough to distinguish the two. The measurement of the $B(E2)$ between the odd-spin and even-spin members of the wobbling excitations was proposed as a crucial method of discrimination. Even-even nuclei were considered in [41] since the observed one-phonon wobbling band corresponds to the odd-spin members for the even-spin yrast TSD band. In some Lu isotopes the so-called two-phonon wobbling bands have been observed [11,12]. They correspond to the even-spin members of the wobbling excitations in even-even nuclei. The $B(E2)$ values of transitions from the two-phonon to one-phonon wobbling band are measured to be about twice the values of those from the one-phonon wobbling to the yrast band, which clearly fits the picture of the γ-rigid model rather than the γ-soft model. Although the negative γ shape is assumed in Ref. [41], which is believed to be opposite to what is measured in Lu isotopes, the main conclusion is not affected; it confirms the picture of the wobbling mode [7] based on the static triaxial deformation. Thus, it is meaningful to ask how large is the triaxiality of the observed TSD bands.

The paper is organized as follows. Various existing definitions of the triaxiality parameter γ are reviewed, and their values for a given shape are compared in Sec. II. After discussing the difference between the γ values used in the Nilsson-Strutinsky calculations and the particle-rotor model, in Sec. III, it is shown that our RPA calculation gives the correct magnitude of the $B(E2)$ ratios if the same triaxial deformation parameter is used as in the analysis of the rotor model in Ref. [8]. Section IV is devoted to the summary. A part of the present work was presented in some conference reports [42,43].

II. PARAMETRIZATIONS OF TRIAXIAL DEFORMATION

The size of triaxial deformation is usually designated by the triaxiality parameter γ, but there are various definitions for it. In this section, we discuss the relationship between them and show how much their differences are for a given shape. It should be mentioned that this problem has already been discussed in Ref. [44] (Appendix B) for the volume-conserving anisotropic harmonic oscillator potential. The present study generalizes the discussion to more realistic potentials.

A. Basic definition based on the intrinsic quadrupole moments

One of the most important characteristics of nuclei with static triaxial deformation is the existence of two distinct intrinsic quadrupole moments. We take the intrinsic z-axis as the axis of quantization and the x-axis as the axis of rotation, and define the two moments [7],

$$\begin{cases} Q_0 \equiv \sqrt{\frac{16\pi}{5}}\langle \hat{Q}_{20}\rangle = \int (2z^2 - x^2 - y^2)\rho(\boldsymbol{r})d^3\boldsymbol{r}, \\ Q_2 \equiv \sqrt{\frac{16\pi}{5}}\langle \hat{Q}_{22}\rangle = \sqrt{\frac{3}{2}}\int (x^2 - y^2)\rho(\boldsymbol{r})d^3\boldsymbol{r}, \end{cases} \tag{1}$$

where $\langle \hat{Q}_{2K}\rangle$ is the expectation value of the usual quadrupole operator in the intrinsic frame of the deformed nucleus, and $\rho(\boldsymbol{r})$ is the corresponding nucleonic density. These two moments are directly related to the in-band and out-of-band $B(E2)$ values of the wobbling band [7], the measurements of which can uniquely determine the moments as has actually been done in the case of the Lu isotopes [21,22]. In place of the two moments, equivalent two quantities, the magnitude of moments Q and the triaxiality parameter γ are usually used:

$$Q_0 = Q\cos\gamma, \quad -\sqrt{2}\,Q_2 = Q\sin\gamma. \tag{2}$$

Here we follow the Lund convention [17] for the sign of γ, which is opposite to that of Ref. [7].

The triaxiality parameter defined above reflects the nuclear density distribution $\rho(\boldsymbol{r})$ and we call it "γ(den)" in this work, i.e.,

$$\tan\gamma(\text{den}) = -\frac{\sqrt{2}\langle \hat{Q}_{22}\rangle}{\langle \hat{Q}_{20}\rangle}. \tag{3}$$

Theoretical calculation of γ(den) with $\rho(\boldsymbol{r})$ depends on the assumed single-particle wave functions and shell model configuration of the nucleus. It is sometimes more convenient to introduce another parameter "γ(geo)" which is more directly related to the geometric shape of the nucleus

$$\tan\gamma(\text{geo}) = -\frac{\sqrt{2}\langle \hat{Q}_{22}\rangle_{\text{uni}}}{\langle \hat{Q}_{20}\rangle_{\text{uni}}}, \tag{4}$$

where $\langle\,\rangle_{\text{uni}}$ means that the expectation value in Eq. (1) is taken with respect to the sharp-cut uniform density distribution within a properly defined two dimensional surface Σ specifying the nuclear shape

$$\rho_{\text{uni}}(\boldsymbol{r}) \equiv \begin{cases} \rho_0 & \text{for } \boldsymbol{r} \text{ inside the surface } \Sigma, \\ 0 & \text{otherwise.} \end{cases} \tag{5}$$

If the triaxial density distribution is calculated with an average single-particle potential, whose equipotential surface Σ specifies the nuclear shape, then the two triaxiality parameters, γ(den) and γ(geo), agree very well. In Fig. 1 an example of the ratio γ(den)/γ(geo) is plotted as a function of γ(geo) for the TSD nuclei ^{163}Lu calculated with a Nilsson and a Woods-Saxon potentials; the precise definition of the surface for each potential is given in the following subsections. γ(den) and γ(geo) coincide typically within 10% except in the small γ region where both of them approach zero and the ratio is numerically unstable. This agreement corresponds to the so-called shape consistency between the density and the potential [45], which has been tested both for a Nilsson and a Woods-Saxon potential for axially symmetric deformations [46,47]. The agreement shows that the consistency is valid also for triaxial deformation, and allows one to use γ(geo) in place of γ(den) in practice.

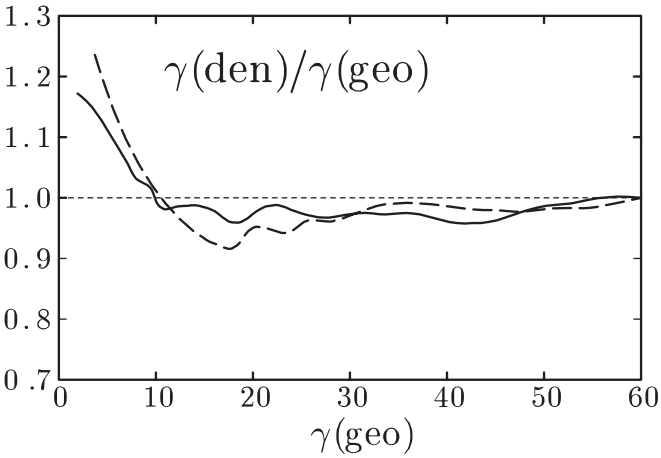

FIG. 1. The ratios $\gamma(\text{den})/\gamma(\text{geo})$ are plotted as functions of $\gamma(\text{geo})$ for the cases of a triaxially deformed Nilsson (solid curve) and Woods-Saxon potentials (dashed curve). Calculations have been performed for the TSD band in ^{163}Lu, and the parameters used for the Nilsson potential are $\epsilon_2 = 0.43$, $\epsilon_4 = 0.0$, and those for the Woods-Saxon potential are $\beta_2 = 0.42$, $\beta_4 = 0.034$, which has almost the same shape as the case of the Nilsson potential at $\gamma(\text{geo}) \approx 10^\circ$ at the minimum of the potential energy surface in the Nilsson-Strutinsky calculation. The pairing gap parameters $\Delta_{\text{n,p}} = 0.3$ MeV are used in both cases.

In the microscopic calculations by means of the Hartree-Fock(-Bogoliubov) method, there is no predefined shape, and $\gamma(\text{den})$ is the most natural parameter to represent the triaxiality. In the case of the Strutinsky method, however, one starts from some average nuclear potential, and calculates the potential energy surface or the total Routhian surface to determine the self-consistent deformation. In this case, the potential is parametrized by a different kind of parameter, γ, to conveniently specify a predefined shape of the potential. We call this third type of definition "γ(pot)": In the following, we consider two conventionally used definitions, depending on the employed potential.

B. γ(pot) used in the Nilsson potential

As a definite example of γ(pot), we take the one calculated with a Nilsson (modified oscillator) potential, i.e., γ(pot:Nils). The deformation parameters in the Nilsson potential [17, 48,49] considered in the present work are $(\epsilon_2, \gamma, \epsilon_4)$ with $\gamma = \gamma(\text{pot:Nils})$ which define the deformation of the velocity independent part of potential through the single-stretched coordinate, $\boldsymbol{r}' \equiv (\sqrt{\omega_x/\omega_0}\, x, \sqrt{\omega_y/\omega_0}\, y, \sqrt{\omega_z/\omega_0}\, z)$, as

$$V(\boldsymbol{r}) = \frac{1}{2} M\omega_0\omega_{\text{v}}(\epsilon_2, \gamma, \epsilon_4) r'^2 \times \left(1 - \sum_{K=0,\pm2} c_{2K} Y_{2K}(\Omega') - \sum_{K=0,\pm2,\pm4} c_{4K} Y_{4K}(\Omega')\right), \tag{6}$$

where ω_0 is the frequency of the spherical potential, $\omega_{\text{v}}(\epsilon_2, \gamma, \epsilon_4)$ is determined by the volume conserving condition, and Ω' is the solid-angle of coordinate $\boldsymbol{r}'$. The coefficients c's are given by

$$\begin{cases} c_{20} = \sqrt{\frac{16\pi}{45}}\, \epsilon_2 \cos\gamma, \\ c_{22} = c_{2-2} = -\sqrt{\frac{8\pi}{45}}\, \epsilon_2 \sin\gamma, \\ c_{40} = \frac{\sqrt{4\pi}}{9}\, \epsilon_4 (5\cos^2\gamma + 1), \\ c_{42} = c_{4-2} = -\frac{\sqrt{120\pi}}{9}\, \epsilon_4 \cos\gamma \sin\gamma, \\ c_{44} = c_{4-4} = \frac{\sqrt{70\pi}}{9}\, \epsilon_4 \sin^2\gamma. \end{cases} \tag{7}$$

The nuclear shape Σ is defined as an equipotential surface, $V(\boldsymbol{r}) = \text{const.}$, and is uniquely determined by the parameters $(\epsilon_2, \gamma, \epsilon_4)$ independent of the constant. The triaxiality parameters $\gamma(\text{den})$ and $\gamma(\text{geo})$ defined in the previous subsection can be calculated as functions of $(\epsilon_2, \gamma = \gamma(\text{pot:Nils}), \epsilon_4)$. The three frequencies, ω_x, ω_y, and ω_z, are given by Eq. (9) below.

As is already shown in Fig. 1, $\gamma(\text{den})$ and $\gamma(\text{geo})$ are very similar. Therefore we compare $\gamma(\text{geo})$ and $\gamma(\text{pot:Nils})$ in Fig. 2 in three cases with $\epsilon_2 = 0.2, 0.4, 0.6 (\epsilon_4 = 0)$. As the figure shows, we see that the difference between them is large. This implies that the $\gamma(\text{den})$ is quite different from $\gamma(\text{pot:Nils})$ for the TSD band in Lu nuclei where $\epsilon_2 \gtrsim 0.4$; for example $\gamma(\text{pot:Nils}) = 20^\circ$ corresponds to $\gamma(\text{den}) \approx \gamma(\text{geo}) \approx 11^\circ$, so that the difference can be as much as about a factor two. It is also clear that the difference is the larger, the larger is ϵ_2 : $\gamma(\text{geo})$ is only about 10° when $\gamma(\text{pot:Nils})$ is 30° in the case of the superdeformed band, where the deformation is typically $\epsilon_2 \approx 0.6$.

It should be emphasized that the shape of the potential and that of the density are consistent as is discussed in the previous subsection. The parameter $\gamma(\text{pot:Nils})$ is just not appropriate to describe triaxiality of the geometrical shape of the potential.

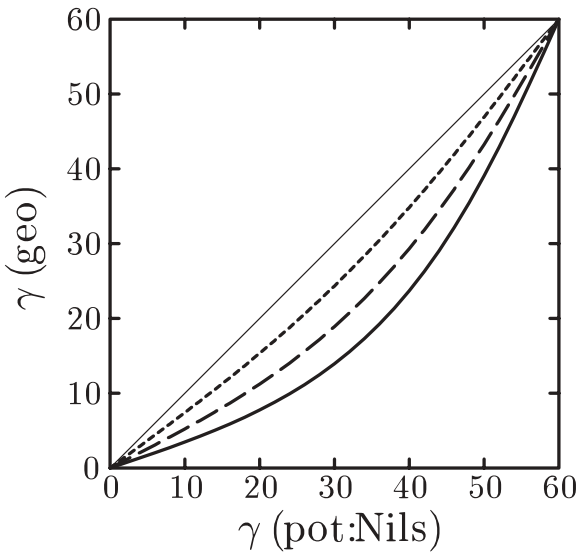

FIG. 2. The values of the triaxiality parameters $\gamma(\text{geo})$ for fixed ϵ_2 and ϵ_4 deformation parameters are shown as functions of $\gamma(\text{pot:Nils})$ (the thin diagonal line is just a guide for the eyes). The dotted curve is for the case with $\epsilon_2 = 0.2$, the dashed with $\epsilon_2 = 0.4$, and the solid with $\epsilon_2 = 0.6$, respectively. The ϵ_4 parameter is set 0 for all the cases.

In the case of $\epsilon_4 = 0$, the Nilsson potential reduces to the anisotropic harmonic oscillator potential except for the $\boldsymbol{l}^2$ and $\boldsymbol{l}\cdot\boldsymbol{s}$ terms, which are irrelevant to the definition of the nuclear shape. It is instructive to consider this case for understanding the difference shown in Fig. 2. The shape of the potential is a volume-conserving ellipsoid defined by simple equations,

$$\sum_{i=1}^{3}\omega_i^2 x_i^2 = \text{const.}, \quad \text{with} \quad \prod_{i=1}^{3}\omega_i = \omega_0^3. \tag{8}$$

The frequencies ω_i $(i = 1, 2, 3)$ for the x, y, z-directions, which are inversely proportional to the lengths of the ellipsoid along these axes, are given by

$$\omega_i = \omega_\nu\left(1 - \frac{2}{3}\epsilon_2\cos\left(\gamma + \frac{2\pi}{3}i\right)\right), \quad \gamma = \gamma(\text{pot:Nils}), \tag{9}$$

and $\tan\gamma(\text{geo})$ and $\tan\gamma(\text{pot:Nils})$ are reduced to

$$\tan\gamma(\text{geo}) = \frac{\sqrt{3}\left(\omega_y^{-2} - \omega_x^{-2}\right)}{2\omega_z^{-2} - \omega_y^{-2} - \omega_x^{-2}}, \tag{10}$$

$$\tan\gamma(\text{pot:Nils}) = \frac{\sqrt{3}\,(\omega_y - \omega_x)}{2\omega_z - \omega_y - \omega_x}, \tag{11}$$

for a given value of ϵ_2. In the limit of small deformation parameters, $\epsilon_2, |\gamma| \ll 1$, it is easy to confirm

$$\gamma(\text{geo}) \approx \left(1 - \frac{3}{2}\epsilon_2\right)\gamma(\text{pot:Nils}). \tag{12}$$

Namely, the slope of curves at the origin in Fig. 2 changes with ϵ_2 with a rather large factor $\frac{3}{2}$, and clearly explains why $\gamma(\text{geo})$ gets smaller relative to $\gamma(\text{pot:Nils})$ as ϵ_2 increases.

In order to see how these different definitions of two triaxiality parameters, $\gamma(\text{geo})$ and $\gamma(\text{pot:Nils})$, change the appearance of potential energy surface, we show an example in Fig. 3. Here the ϵ_4 parameter is chosen to minimize the potential energy at each (ϵ_2, γ) mesh points. The parameter $\gamma(\text{geo})$ depends not only on $(\epsilon_2, \gamma(\text{pot:Nils}))$ but also on ϵ_4, and it is impossible to calculate the $(\epsilon_2, \gamma(\text{geo}))$ mesh points before the minimization with respect to ϵ_4. Therefore, we made an approximation to set $\epsilon_4 = 0$ when we prepared the $(\epsilon_2, \gamma(\text{geo}))$ mesh points from the $(\epsilon_2, \gamma(\text{pot:Nils}))$ mesh points. As is clear from the figure, the surface is squeezed to the $\gamma = 0$ axis at larger deformation, and apparently the TSD minimum moves to smaller triaxial values. In Fig. 3, only the γ parameter is changed from $\gamma(\text{pot:Nils})$ to $\gamma(\text{geo})$. However, it may be better to replace also ϵ_2 by another parameter corresponding to the magnitude of Q in Eq. (2), e.g. $\beta = \sqrt{\frac{4\pi}{5}}\,Q/\langle\sum_{k=1}^{A}\boldsymbol{r}^2\rangle$, in order to make the meaning of the quadrupole deformation clearer. Since, however, constraint Hartree-Fock(-Bogoliubov) type calculations are necessary for such a purpose, the simplicity of the Strutinsky type calculation may be lost.

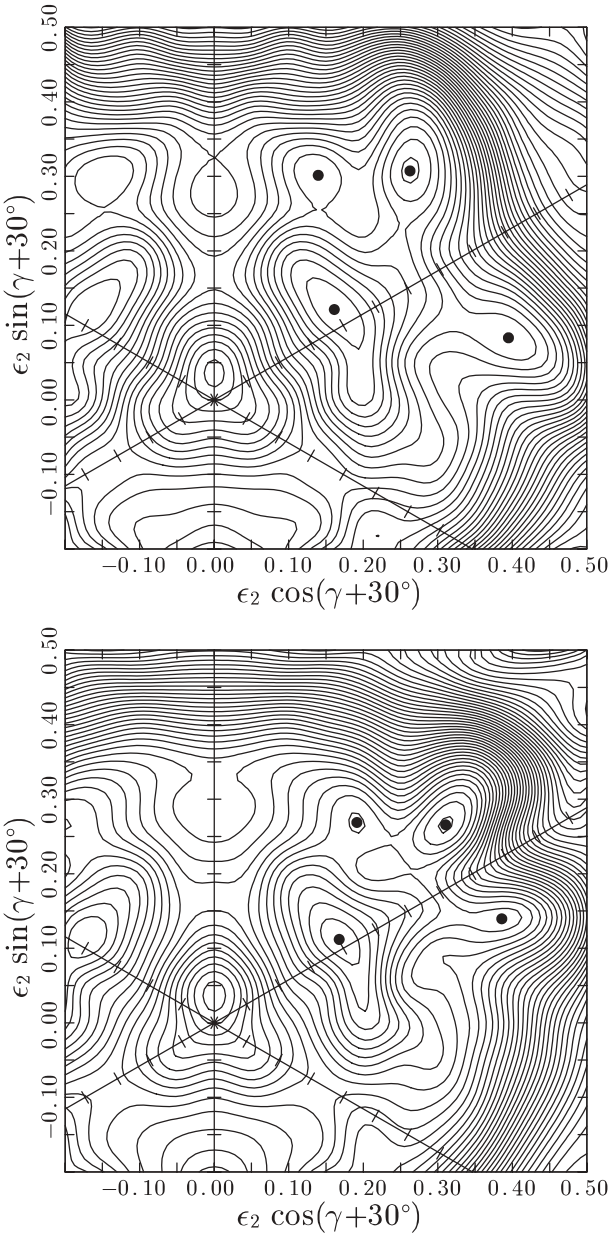

FIG. 3. Potential energy surface obtained by the cranked Nilsson-Strutinsky calculation for the $(\pi, \alpha) = (+, +1/2)$ configuration in ^{163}Lu at $I = 41/2^+$. The energy between contours is 250 keV. The triaxiality parameter $\gamma = \gamma(\text{pot:Nils})$ is used as usual in the upper panel, while $\gamma = \gamma(\text{geo})$ is used in the lower panel.

C. γ(pot) used in the Woods-Saxon potential

As another example of $\gamma(\text{pot})$, the one for a deformed Woods-Saxon potential is considered, i.e., $\gamma(\text{pot:WS})$. Actually, the discussion is not restricted to the Woods-Saxon potential, but is more general. The deformed Woods-Saxon potential considered in this work is parametrized by $(\beta_2, \gamma, \beta_4)$, with $\gamma = \gamma(\text{pot:WS})$, and defined [50–52] by

$$V(\boldsymbol{r}) = \frac{V_0}{1 + \exp(\text{dist}_\Sigma(\boldsymbol{r})/a)}, \tag{13}$$

where $\text{dist}_\Sigma(\boldsymbol{r})$ is the distance between a given point $\boldsymbol{r}$ and the nuclear surface Σ (with a minus sign if $\boldsymbol{r}$ is inside Σ), whose

radius in the direction Ω from the origin is given by $r = R(\Omega)$;

$$R(\Omega) = R_{\rm v}(\beta_2, \gamma, \beta_4) \times \left(1 + \sum_{K=0,\pm2} a_{2K} Y_{2K}(\Omega) + \sum_{K=0,\pm2,\pm4} a_{4K} Y_{4K}(\Omega)\right), \quad (14)$$

where $R_{\rm v}(\beta_2, \gamma, \beta_4)$ is determined by the volume conservation condition, and the coefficients a's are given by

$$\begin{cases} a_{20} = \beta_2 \cos\gamma, \\ a_{22} = a_{2-2} = -\frac{1}{\sqrt{2}} \beta_2 \sin\gamma, \\ a_{40} = \frac{1}{6} \beta_4 (5\cos^2\gamma + 1), \\ a_{42} = a_{4-2} = -\sqrt{\frac{5}{6}} \beta_4 \cos\gamma \sin\gamma, \\ a_{44} = a_{4-4} = \sqrt{\frac{35}{72}} \beta_4 \sin^2\gamma. \end{cases} \quad (15)$$

The surface Σ is an equipotential surface at the half depth, $V(\boldsymbol{r}) = \frac{1}{2} V_0$, and is directly related to $(\beta_2, \gamma, \beta_4)$ by $\gamma = \gamma$(pot:WS).

Figure 4 shows the relation between γ(geo) and γ(pot:WS) for three different cases of (β_2, β_4) deformations, corresponding to Fig. 2. Although the difference between γ(geo) and γ(pot:WS) is not so dramatic as between γ(geo) and γ(pot:Nils), it is still considerably large. Again, since γ(den) and γ(geo) are very similar as shown in Fig. 1, this means that γ(den) is quite different from γ(pot:WS) for the TSD band in the Lu region: γ(den) $\approx \gamma$(geo) $\approx 13^\circ$ when γ(pot:WS) $= 20^\circ$. In the case of the parametrization of the nuclear surface

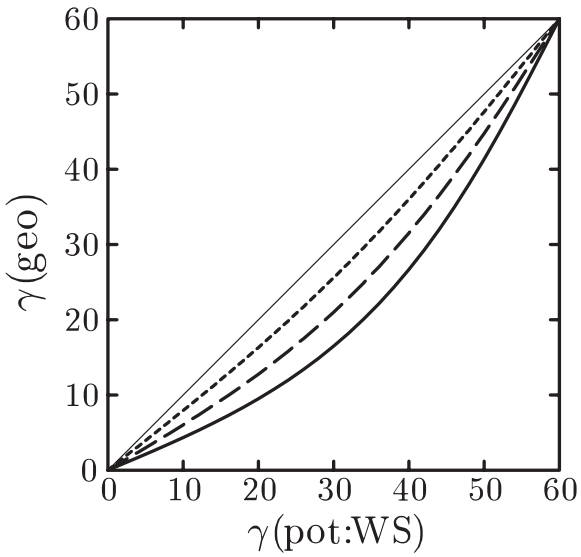

FIG. 4. The triaxiality parameters γ(geo) with fixed β_2 and β_4 deformation parameters are shown as functions of γ(pot:WS) (the thin diagonal line is a guide for the eyes). The dotted curve is for $\beta_2 = 0.217$ and $\beta_4 = 0.017$, the dashed curve for $\beta_2 = 0.445$ and $\beta_4 = 0.075$, and the solid curve for $\beta_2 = 0.685$ and $\beta_4 = 0.190$, respectively. These sets of parameters correspond to the cases of $\epsilon_2 = 0.2$, $\epsilon_2 = 0.4$, and $\epsilon_2 = 0.6$ with $\epsilon_4 = 0$ in the case of the Nilsson potential in Fig. 2 at γ(geo) $= 0$.

in Eq. (14), $\langle \hat{Q}_{2K} \rangle_{\rm uni}$ can be easily calculated

$$\langle \hat{Q}_{2K} \rangle_{\rm uni} = \frac{1}{5} \rho_0 \int R(\Omega)^5 Y_{2K}(\Omega) d\Omega. \quad (16)$$

Then, it is straightforward to see that for $\beta_4 = 0$ in the small deformation limit, $\beta_2, |\gamma| \ll 1$,

$$\gamma(\text{geo}) \approx \left(1 - \sqrt{\frac{180}{49\pi}} \beta_2\right) \gamma(\text{pot:WS}). \quad (17)$$

Taking into account the relation, $\beta_2 \approx \sqrt{\frac{16\pi}{45}} \epsilon_2$ in the small deformation limit, the proportionality constant in front of ϵ_2 corresponds to $\sqrt{\frac{180}{49\pi}} \times \sqrt{\frac{16\pi}{45}} = \frac{8}{7} \approx 1.14$ which is quite large, though smaller than $\frac{3}{2} = 1.5$ in Eq. (12) for the Nilsson potential. This explains qualitatively the increase of the difference between γ(geo) and γ(pot:WS) for larger deformation in Fig. 4. Thus, again, the parameter γ(pot:WS) is not appropriate for describing the triaxial shape of the potential.

III. $B(E2)$ RATIO OF THE WOBBLING BAND

The two intrinsic quadrupole moments in the previous section are related to the two kinds of $B(E2)$'s, i.e., $B(E2)_{\rm in}$ for the $\Delta I = -2$ intraband $E2$ transitions within the wobbling band, and $B(E2)_{\rm out}$ for the $\Delta I = \pm 1$ interband $E2$ transitions from the one-phonon wobbling band to the yrast TSD band. The measurements of both the branching ratio and the life time have been done for some TSD bands [21,22] recently, so that one can study $B(E2)_{\rm out}$ and $B(E2)_{\rm in}$ separately. However, their ratio is directly connected to the triaxial deformation in the high-spin wobbling phonon treatment of the rotor model [7], which gives, in good approximation,

$$\frac{B(E2; I \to I \pm 1)_{\rm out}}{B(E2; I \to I - 2)_{\rm in}} \approx \frac{2}{I} \left(\frac{w_z \sin(\gamma + 60^\circ) \mp w_y \sin\gamma}{\sqrt{w_y w_z} \cos(\gamma + 30^\circ)}\right)^2, \quad \gamma = \gamma(\text{den}), \quad (18)$$

where the quantities w_y, w_z are related to the three moments of inertia, $\mathcal{J}_x, \mathcal{J}_y$, and $\mathcal{J}_z$, through

$$\begin{cases} w_y \equiv (\mathcal{J}_x/\mathcal{J}_z - 1)^{1/2}, \\ w_z \equiv (\mathcal{J}_x/\mathcal{J}_y - 1)^{1/2}. \end{cases} \quad (19)$$

Note that the $I \to I + 1$ transitions are quenched for the positive γ shape, and in fact only the $I \to I - 1$ transitions are observed in Lu nuclei. We concentrate on the $B(E2)$ ratio in the following.

In Fig. 5, the experimental $B(E2)$ ratio of the one-phonon wobbling band in ^{163}Lu [22] is compared with the results of the particle-rotor model calculation. We take five values of γ(den) $= 10^\circ, 15^\circ, 20^\circ, 25^\circ$, and 30° to show the dependence of the $B(E2)$ ratio on the γ values. All the other parameters are taken from Ref. [24]. While the existence of the odd proton brings about important corrections to the energy spectra, its effect on the $B(E2)$ is very small [24,53]. In fact, the results of the calculation, dotted curves in the figure, can be understood nicely by the simple expression in Eq. (18) for even-even nuclei: The decrease of the $B(E2)$ ratio as a function of spin

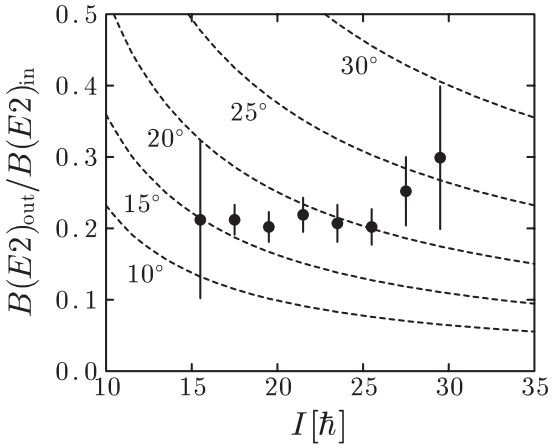

FIG. 5. The $B(E2)$ ratio, $B(E2; I \to I-1)_{\rm out}/B(E2; I \to I-2)_{\rm in}$, of the wobbling band in ^{163}Lu. The experimental data [22] are compared with the calculation by the particle-rotor model [24]. Five dotted curves are, from the bottom to the top, the results with the triaxiality parameter $\gamma(\text{den}) = 10^\circ, 15^\circ, 20^\circ, 25^\circ$, and 30°, respectively.

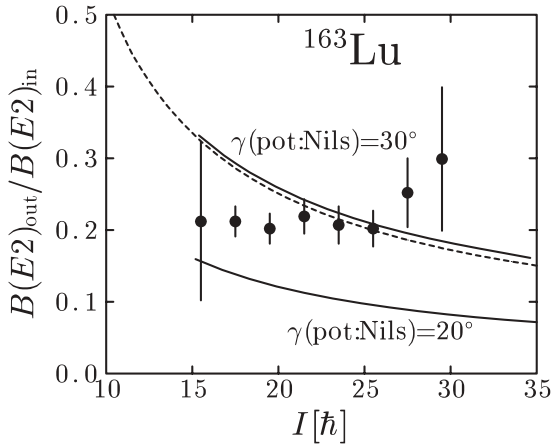

FIG. 6. The $B(E2)$ ratio, $B(E2; I \to I-1)_{\rm out}/B(E2; I \to I-2)_{\rm in}$, of the one-phonon wobbling band in ^{163}Lu. The experimental data [22] are compared with our microscopic RPA calculations. The lower solid curve is the result with $\gamma = \gamma(\text{pot:Nils}) = 20^\circ$, while the upper solid curve is with $\gamma(\text{pot:Nils}) = 30^\circ$; the full model space is used for both of them. The dotted curve is the same as that in Fig. 5, viz. the result of the particle-rotor calculation with $\gamma = \gamma(\text{den}) = 20^\circ$, shown for reference.

is due to the $1/I$ dependence if all the model parameters are held fixed, and the ratio increases quickly as $\gamma = \gamma(\text{den})$ is increased. Although the spin-dependence calculated by the particle-rotor model does not agree with the experimental data, the average magnitude of the $B(E2)$ ratio indicates that the size of triaxiality of ^{163}Lu is $\gamma = \gamma(\text{den}) \approx 20^\circ$, which is one of the main conclusions of Ref. [24]. This conclusion remains valid even if other parameters, such as the moments of inertia, are changed within a reasonable range.

It may also be interesting to note that the measured $B(E2)$ ratio is almost constant and even increases as spin approaches its highest value. This strongly suggests that the triaxiality parameter $\gamma = \gamma(\text{den})$ is not constant and increases with spin [24] among other parameters. A preliminary investigation for such a possibility has been reported in Ref. [43], where microscopic framework of the cranked Woods-Saxon mean-field and the random phase approximation (RPA) is employed.

Next let us turn to the discussion on our microscopic calculations in Refs. [25–27] based on cranked Nilsson mean-field and RPA. In those calculations the triaxiality parameter $\gamma = 20^\circ$ was employed but the resultant $B(E2)$ ratios were too small; we have been wondering why the results of RPA calculation deviate so much from those of the rotor model. It has been shown in Ref. [54] that RPA calculation reproduces the result of the rotor model rather well in the case of the precession bands built upon the high-K isomers, which can be interpreted as a similar motion to the wobbling excitation, in which the angular momentum vector fluctuates about the main rotation axis [55]. Now the reason for the small calculated $B(E2)$ ratio is clear from the argument of the previous section: The triaxiality parameter used in our calculations is that of the Nilsson potential, $\gamma = \gamma(\text{pot:Nils})$, of Sec. II B, while $\gamma = \gamma(\text{den})$ of Sec. II A is used in the rotor model. Their difference is large. In order to perform the equivalent calculation as the rotor model with $\gamma(\text{den}) \approx 20^\circ$, one has to employ $\gamma(\text{pot:Nils}) \approx 30^\circ$ according to the result of the previous section. It should also be mentioned that we have used five major oscillator shells, $N_{\rm osc} = 2$–6 for protons and $N_{\rm osc} = 3$–7 for neutrons in the calculation in Refs. [25–27], but they were not enough; since the $i_{13/2}$ proton orbits are occupied in the TSD band, $N_{\rm osc} = 8$ proton quasiparticle states need be included in the RPA calculation.

In Fig. 6 we show the new results of calculation with $\gamma(\text{pot:Nils}) = 20^\circ$ and 30° with the full model space; all orbits in the oscillator shell $N_{\rm osc} = 0$–9 for both protons and neutrons are included. The procedure and other parameters in the calculation are the same as in the previous work [25]; $\epsilon_2 = 0.43$, $\epsilon_4 = 0$, and the pairing gaps $\Delta_{\rm n,p} = 0.3$ MeV. The particle-rotor model with $\gamma(\text{den}) = 20^\circ$ (the dotted curve) is also included. The underestimation of our previous result is partly because of the small model space (about 20%, see Ref. [54]), but the main reason is due to the fact that we have used $\gamma = \gamma(\text{pot:Nils}) = 20^\circ$, which corresponds to much smaller triaxiality than $\gamma(\text{den}) = 20^\circ$ in the particle-rotor model. The result with $\gamma(\text{pot:Nils}) = 30^\circ$ almost coincides with that of the particle-rotor calculation with $\gamma(\text{den}) = 20^\circ$. This is because the values of the microscopically calculated moments of inertia accidentally take similar values in the relevant spin range [25].

In order to see the γ dependence, we show in Fig. 7 the $B(E2)$ ratio and the excitation energy of the one-phonon wobbling band in ^{163}Lu at spin $I = 51/2$ as functions of the triaxiality $\gamma = \gamma(\text{pot:Nils})$. Although the excitation energy is rather flat in the range, $20^\circ \leqslant \gamma(\text{pot:Nils}) \leqslant 30^\circ$, the $B(E2)$ follows the behaviors of Eq. (18) if the relation between $\gamma(\text{pot:Nils})$ and $\gamma(\text{den})$ is taken into account. The excitation energy can be expressed in terms of the three moments of inertia in a usual way [7,30], but their γ dependence is not like the irrotational inertia [37,40], which leads to the rather weak γ dependence of the excitation energy. Here we have only shown the example of the wobbling excitation in ^{163}Lu, but

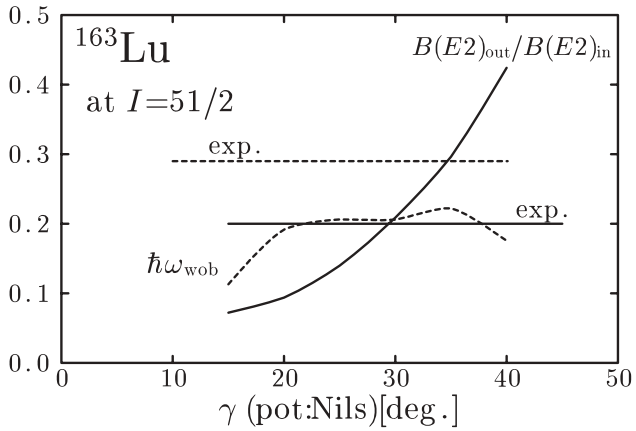

FIG. 7. The γ dependence of the microscopically calculated $B(E2)$ ratio and the excitation energy of the one-phonon wobbling band in ^{163}Lu at spin $I = 51/2$. The solid curve is for the $B(E2)$ ratio and the dotted curve for the energy in MeV. The horizontal solid and dotted lines designate the experimental values.

we have confirmed that these properties of the wobbling-like RPA solution are general, and can be applied to other cases in the Lu region.

Thus, it is confirmed that in the Lu region RPA and macroscopic rotor model predict the same behavior of $B(E2)$'s; namely the out-of-band $B(E2)$ can be related to the intrinsic quadrupole moments by Eq. (1). This is nontrivial in practice since it allows the out-of-band $B(E2)$ to be calculated by the RPA transition amplitudes of the nondiagonal part of the quadrupole operators, $Q_{21}^{(-)}$ and $Q_{22}^{(-)}$ [28,30]. It has been shown [37] that the RPA wobbling theory of Marshalek [30] gives the same expression of the out-of-band $B(E2)$ as that of the rotor model, if the RPA wobbling mode is collective enough so that the quantity "c_n" defined in Eq. (4.29) in Ref. [37] satisfies $c_{n=\mathrm{wob}} = 1$. In the previous calculations [25–27,37], the employed model space was too small[1] to give $c_{n=\mathrm{wob}} = 1$, but we have confirmed that it is satisfied within 1% in the present full model space calculations. Recently, this criterion, $c_{n=\mathrm{wob}} \approx 1$, has been used to identify the wobbling-like solution out of many RPA eigenmodes, and shown to be very useful [39].

IV. SUMMARY

In this work, we first discussed various definitions of the triaxiality parameter γ. The most basic ones among them are those defined through the two intrinsic quadrupole moments, γ(den) defined by Eq. (3) for each configuration of the particular nucleus considered, and γ(geo) defined by Eq. (4) for a given shape of potential. These two definitions are found to coincide in good approximation: The nuclear shape consistency between the potential and density holds. In Hartree-Fock(-Bogoliubov) type calculations, where the nuclear mean-field is determined self-consistently by a suitably chosen effective interaction, the parameter γ(den) is the only natural definition of the measure of triaxial deformation. However, in the Strutinsky type macroscopic-microscopic method, where one starts from a predefined average potential, triaxiality parameters can be introduced in various ways. In this work, the two widely used ones are investigated: The Nilsson type parametrization γ(pot:Nils) in Eqs. (6) and (7) and the Woods-Saxon type parametrization γ(pot:WS) in Eqs. (13) and (14) are compared with the density type γ(geo). The difference between the potential type and the density type γ's, e.g., γ(pot:Nils) vs. γ(geo), is particularly conspicuous for states with larger deformations, e.g., the triaxial superdeformed states. Thus, the potential type parametrizations are not suitable for representing the actual triaxiality of the density type, and one has to be very careful about which definition is used in the discussions of the triaxiality.

Next investigated is the out-of-band to in-band $B(E2)$ ratio of the one-phonon wobbling band, which is measured systematically in the Lu region and is sensitive to the triaxial deformation. The macroscopic particle-rotor model [24] is used to deduce the triaxial deformation from the experimental $B(E2)$ ratio, which leads to $\gamma = \gamma(\mathrm{den}) \approx 20^\circ$ on average. On the other hand, microscopic RPA calculation [25,26] using $\gamma = \gamma(\mathrm{pot:Nils}) \approx 20^\circ$ obtained for TSD minima in the cranked Nilsson-Strutinsky calculation [19,20], gave too small $B(E2)$ ratio compared with the experimental data. The reason for the underestimate is found to be mainly due to the small triaxiality used: $\gamma(\mathrm{pot:Nils}) \approx 20^\circ$. That corresponds to $\gamma(\mathrm{den}) \approx 11^\circ$, which is much smaller than $\gamma(\mathrm{den}) \approx 20^\circ$ in the particle-rotor model calculations. If the same triaxiality is used, the RPA calculation can well reproduce the magnitude of the measured $B(E2)$ ratio as does the particle-rotor model.

It should, however, be emphasized that an important problem remains: The triaxial deformations, $\gamma(\mathrm{den}) \approx 11^\circ$, predicted by the cranked Nilsson-Strutinsky calculations [19,20] for the TSD bands in the Hf, Lu region are too small to account for the measured $B(E2)$ ratio of the wobbling excitations. We believe that this is a challenge to the existing microscopic theory. Another point we would like to mention is that the measured $B(E2)$, both the out-of-band and in-band $B(E2)$'s, seem to indicate that the triaxial deformation increases at high spins [24]. We have recently developed a new RPA approach [43] based on the Woods-Saxon potential as a mean-field, which is believed to be more reliable than our previous calculations with the Nilsson potential. The result of calculations and discussions on the problem of the spin dependence of the triaxial deformation suggested by the measured $B(E2)$'s will be reported in a subsequent paper; see Ref. [43] for a preliminary report.

[1] In Ref. [27], it was reported that $c_{n=\mathrm{wob}} = 0.6$–0.8, but these values were not correct; they were in the cases with even smaller model spaces. The calculation with the five major shells gives $c_{n=\mathrm{wob}} \approx 0.9$, which leads to about a 20% reduction of $B(E2)_{\mathrm{out}}/B(E2)_{\mathrm{in}}$ as it can be seen by comparing the result of Fig. 3 of Ref. [25] with Fig. 6 of the present paper.

ACKNOWLEDGMENTS

This work was inspired by collaborations on wobbling motion with Prof. K. Matsuyanagi. We thank Prof. M. Kawai for carefully reading and greatly improving the manuscript.

[1] A. S. Davydov and B. F. Filippov, Nucl. Phys. **A8**, 237 (1958).
[2] J. Meyer-ter-Vehn, Nucl. Phys. **A249**, 111, 141 (1975).
[3] D. Cline, Annu. Rev. Nucl. Part. Sci. **36**, 683 (1986).
[4] W. Andrejtscheff and P. Petkov, Phys. Lett. **B329**, 1 (1994).
[5] I. Hamamoto, in *Proceedings of the Workshop on Microscopic Models in Nuclear Structure Physics, Oak Ridge, USA, October 3–6, 1988*, edited by M. W. Guidry *et al*. (World Scientific, Singapore, 1989), p. 173.
[6] I. Hamamoto, Nucl. Phys. **A520**, 297c (1990).
[7] A. Bohr and B. R. Mottelson, *Nuclear Structure*, Vol. II (Benjamin, New York, 1975).
[8] S. W. Ødegård *et al*., Phys. Rev. Lett. **86**, 5866 (2001).
[9] D. R. Jensen *et al*., Nucl. Phys. **A703**, 3 (2002).
[10] D. R. Jensen *et al*., Eur. Phys. J. A **19**, 173 (2004).
[11] D. R. Jensen *et al*., Phys. Rev. Lett. **89**, 142503 (2002).
[12] G. Schönwaßer *et al*., Phys. Lett. **B552**, 9 (2003).
[13] H. Amro *et al*., Phys. Lett. **B553**, 197 (2003).
[14] P. Bringel *et al*., Eur. Phys. J. A **24**, 167 (2005).
[15] I. Ragnarsson, Phys. Rev. Lett. **62**, 2084 (1989).
[16] S. Åberg, Nucl. Phys. **A520**, 35c (1990).
[17] S. G. Nilsson and I. Ragnarsson, *Shapes and Shells in Nuclear Structure* (Cambridge University Press, Cambridge, 1995).
[18] W. Schmitz *et al*., Phys. Lett. **B303**, 230 (1993).
[19] H. Schnack-Petersen *et al*., Nucl. Phys. **A594**, 175 (1995).
[20] R. Bengtsson, http://www.matfys.lth.se/∼ragnar/TSD.html.
[21] G. Schönwaßer *et al*., Eur. Phys. J. A **15**, 435 (2002).
[22] A. Görgen *et al*., Phys. Rev. C **69**, 031301(R) (2004).
[23] I. Hamamoto, Phys. Rev. C **65**, 044305 (2002).
[24] I. Hamamoto and G. B. Hagemann, Phys. Rev. C **67**, 014319 (2003).
[25] M. Matsuzaki, Y. R. Shimizu, and K. Matsuyanagi, Phys. Rev. C **65**, 041303(R) (2002).
[26] M. Matsuzaki, Y. R. Shimizu, and K. Matsuyanagi, Eur. Phys. J. A **20**, 189 (2004).
[27] M. Matsuzaki, Y. R. Shimizu, and K. Matsuyanagi, Phys. Rev. C **69**, 034325 (2004).
[28] E. R. Marshalek, Nucl. Phys. **A275**, 416 (1977).
[29] D. Janssen and I. N. Mikhailov, Nucl. Phys. **A318**, 390 (1979).
[30] E. R. Marshalek, Nucl. Phys. **A331**, 429 (1979).
[31] J. L. Egido, H. J. Mang, and P. Ring, Nucl. Phys. **A339**, 390 (1980).
[32] Y. R. Shimizu and K. Matsuyanagi, Prog. Theor. Phys. **70**, 144 (1983).
[33] Y. R. Shimizu and K. Matsuyanagi, Prog. Theor. Phys. **72**, 799 (1984).
[34] J. Kvasil and R. G. Nazmitdinov, Phys. Rev. C **69**, 031304(R) (2004).
[35] J. Kvasil and R. G. Nazmitdinov, Phys. Rev. C **73**, 014312 (2006).
[36] M. Matsuzaki, Nucl. Phys. **A509**, 269 (1990).
[37] Y. R. Shimizu and M. Matsuzaki, Nucl. Phys. **A588**, 559 (1995).
[38] D. Almehed, R. G. Nazmitdinov, and F. Dönau, Phys. Scr. T **125**, 139 (2006).
[39] J. Kvasil and R. G. Nazmitdinov, Phys. Lett. **B650**, 331 (2007).
[40] M. Matsuzaki and S.-I. Ohtsubo, Phys. Rev. C **69**, 064317 (2004).
[41] R. F. Casten, E. A. McCutchan, N. V. Zamfir, C. W. Beausang, and J. Y. Zhang, Phys. Rev. C **67**, 064306 (2003).
[42] Y. R. Shimizu, M. Matsuzaki, and K. Matsuyanagi, Phys. Scr. T **125**, 134 (2006).
[43] T. Shoji and Y. R. Shimizu, Int. J. Mod. Phys. E **15**, 1407 (2006).
[44] Y. R. Shimizu and K. Matsuyanagi, Prog. Theor. Phys. **71**, 960 (1984).
[45] B. Nerlo-Pomorska and K. Pomorski, Nukleonika **22**, 289 (1977).
[46] J. Dudek, W. Nazarewicz, and P. Olanders, Nucl. Phys. **A420**, 285 (1984).
[47] R. Bengtsson, J. Dudek, W. Nazarewicz, and P. Olanders, Phys. Scr. **39**, 196 (1989).
[48] S. G. Nilsson, C. F. Tsang, A. Sobiczewski, Z. Szymanski, S. Wycech, C. Gustafsson, I. L. Lamm, P. Möller, and B. Nilsson, Nucl. Phys. **A131**, 1 (1969).
[49] T. Bengtsson and I. Ragnarsson, Nucl. Phys. **A436**, 14 (1985).
[50] J. Dudek, A. Majhofer, J. Skalski, T. Werner, S. Cwiok, and W. Nazarewicz, J. Phys. G **5**, 1359 (1979).
[51] S. G. Rohozinski and A. Sobiczewski, Acta Phys. Pol. B **12**, 1001 (1981).
[52] W. Nazarewicz and A. Sobiczewski, Nucl. Phys. **A369**, 396 (1981).
[53] K. Tanabe and K. Sugawara-Tanabe, Phys. Rev. C **73**, 034305 (2006).
[54] Y. R. Shimizu, M. Matsuzaki, and K. Matsuyanagi, Phys. Rev. C **72**, 014306 (2005).
[55] G. Andersson, S. E. Larsson, G. Leander, P. Möller, S. G. Nilsson, I. Ragnarsson, S. Åberg, J. Dudek, B. Nerlo-Pomorska, K. Pomorski, and Z. Szymanski, Nucl. Phys. **A268**, 205 (1976).